Nigerian Journal of Theoretical and Environmental Physics (NJTEP)
ISSN Print: 3026-9601
DOI: https://doi.org/10.62292/njtep.v2i2.2024.52
Volume 2(2), June 2024

Theoretical Study of Exciton Properties of Dilute GaInAsN Semiconductors

***Uwaoma, C. J., Oriaku, C. l., Joseph, U. and Nnanna, L. A.**

Theoretical and Computational Physics Group, Department of Physics, Michael Okpara University of Agriculture, Umudike

*Corresponding author's email: uwaoma.chinkata@mouau.edu.ng

ABSTRACT

In this research, the electronic band structure, electronic properties and the exciton binding energy of dilute quaternary GaInAsN alloy semiconductors are investigated. This study was aimed to theoretically study the exciton properties of dilute GaInAsN semiconductors. The effects of Nitrogen incorporation in InGaAs alloy was studied within the band anti-crossing model (BAC). The pseudopotential inputs within the virtual crystal approximation (VCA) was employed to make modifications for the nitrogen and indium related alloy disorder effects. The Harrison's model used to study the bandstructure. In general, the results of our computations are in agreement with recent experimental findings. It is found that the presence of nitrogen in the GaInAsN alloy reduces the fundamental bandgap energy within the band anticrossing (BAC) model in the vicinity of the first Brillouin zone boundary, $-\pi/a$to π/a. The heavy hole and electron effective masses, reduced mass, energy band gap, high frequency dielectric constant, static dielectric constant, the refractive indices, polarity, covalency, Bohr radius and binding energy are also modified by the nitrogen and indium fractions of the alloy. For all the alloy compositions studied, it was observed that the binding energies of the excitons vary between the values for InAs$\sim$0.7540 meV and GaAs$\sim$6.0824 meV. Also, the corresponding excitons Bohr radii vary between the values for InAs$\sim$404.4806 Å and GaAs$\sim$105.4916 Å. The information derived from the present study predicts that GaInAsN tunable binding energies and electronic properties are of great technological importance for mid-infrared (MIR) optoelectronics.

Keywords:
Bandstructure,
GaInAsN semiconductor,
Band anticrossing,
Pseudopotential,
Exciton Binding Energy.

INTRODUCTION

In semiconductors, an exciton is the bound state of an electron and a hole. It is every semiconductor system's fundamental optical excitation. It shares many characteristics with atomic hydrogen. Excitonic effects from optical, quantum-optical, and thermodynamic transitions are of interest to researchers because excitons have the potential to condense into a quantum-degenerate state. (Shhri *et al.,* 2011).

The energy necessary to separate an electron from a positively charged hole in a substance is known as the exciton binding energy. It is the cohesive force of an exciton. An exciton is a bound state of an electron and a hole created when an electron is excited to a higher energy level (Chiessa *et al.,* 2020). The exciton's stability is dictated by its binding energy; a higher binding energy indicates a more tightly bound and less likely to dissociate exciton (Baaziz *et al.,* 2012). The dynamics of charge carriers are influenced by nitrogen's incorporation of localized states inside the band structure (Gungerich *et al.,* 2006). The inclusion of N in GaInAsN might result in a complicated interaction between the lattice distortion and charge carrier localization. The exciton effects in GaInAsN enhances its performance in optoelectronic devices for example lasers and photodetector (Stier and Bimberg, 2017).

Specifically, the study estimated the optoelectronic properties such as: refractive index, static and high frequency dielectric constants of GaInAsN alloy using the Harrison's model, calculated the electronic exciton binding energy and Bohr radius of GaInAsN semiconductors, calculated some other semiconductor properties of the dilute GaInAsN such as: polarity and covalency using peudopotential parameters, investigated the effect of nitrogen incorporation on the band parameter, optoelectronic properties as well as the

exciton binding energy and Bohr radius of the dilute GaInAsN semiconductors as well as the effect of band non-parabolicity on the exciton binding energy of the dilute GaInAsN semiconductors.

Theory and Numerical Simulation

The time independent Schrodinger equation, having electrons and holes coordinates r_e and r_h respectively in bulk semiconductors with parabolic $E-k$ dispersion reads,

$$\left[E_g - \frac{\hbar^2}{2m_e^*}\nabla_e^2 - \frac{\hbar^2}{2m_h^*}\nabla_h^2 - \frac{e^2}{4\pi\epsilon(r_e-r_h)}\right]\Psi(r_e,r_h) = E\Psi(r_e,r_h) \quad (1)$$

Where m_e^* and m_h^* are respectively electron and hole effective masses and ε is permittivity of the semiconductor (Harrison, 2005). The Coulumb's interaction between the electron-hole pair is considered to be of hydrogenic type. Hence, it is a standard practice to choose a spherically symmetric wave function $\Psi \sim \exp\left(\frac{-r}{\lambda}\right)$ as the trial wave function, where λ is the variational parameter (Wang *et al.,* 2012). The use of this trial wave function yields in the 3D bulk limit, the ground state exciton Bohr radius and binding energy respectively:

$$a_B = \frac{4\pi\epsilon\hbar^2}{\mu e^2} \quad (2)$$

$$E_B = \frac{\mu e^4}{32\pi^2\hbar^2\epsilon^2} \quad (3)$$

To make modifications for disorder effect, the empirical pseudopotential parameters are defined as a superposition of both local and non-local of pseudo atomic potential of the form

$$V = V_L + V_{NL}. \quad (4)$$

The non-local part has been omitted in this calculation. The pseudopotential Hamiltonian is written as,

$$(H = (h/2m)\nabla^2 + V_L(r) \quad (5)$$

This contains an effective potential which is expanded as Fourier series in reciprocal lattice. The lattice parameter of the dilute quaternary GaInAsN semiconductor obeys the nonlinear interpolation law space (Uma *et al.,* 2016).

$$a_{In_xGa_{1-x}As_{1-y}N_y} = (1-x)(1-y)a_{GaAs} + (1-x)ya_{GaN} + x(1-y)a_{InAs} + xya_{InN} \quad (6)$$

Here a_{GaAs}, a_{GaN}, a_{InAs} and a_{InN} represent the lattice constants of the binary systems of InGaAsN respectively. According to the VCA approximation, the PPFFs for GaInAsN alloys can be given by a sum of nonlinear combinations (Merabet, 2011).

$$V^{s,a}_{Ga_{1-x}In_xAs_{1-y}N_y} = (1-x)(1-y)V^{s,a}_{GaAs} + (1-x)yV^{s,a}_{GaN} + x(1-y)V^{s,a}_{InAs}a_{InAs} + xyV^{s,a}_{InN} \quad (7)$$

The alloy potential is calculated within the VCA approximation. A non-periodic potential $V_{dis}(r)$ due to the compositional disorder is then added to the VCA potential $V_{VCA}(r)$ as

$$V_{alloy}^{(r)} = V_{VCA}^{(r)} + V_{dis}^{(r)} \quad (8)$$

The potential of $In_xGa_{1-x}As_{1-y}N_y$ is determined by taking into account of twokinds of disorder effect, the InGa and the AsN disorders (C_{In-Ga} and C_{As-N}) due to the random distribution of the Ga and In atoms in the cationic sub-lattice and the As and N atoms in the anionic sub-lattice, we obtain for the $V_{alloy}(r)$ the following

$$V_{alloy}(r) = V_{VCA}(r) + V_{1dis}(r) + V_{2dis}(r) \quad (9)$$

$$V_{alloy}(r) = V_{VCA}(r) + x(1-x)C_{In-Ga} + y(1-y)C_{As-N} \quad (10)$$

After developing this later relationship, we obtain $V_{VCA}(r)$ as:

$$V_{VCA}(r) = \left[x^2y\frac{\Omega_{InN}}{\Omega_{alloy}} + xy(1-x)\frac{\Omega_{InAs}}{\Omega_{alloy}}\right]V_{InN(r)} + \left[(1-y)x^2\frac{\Omega_{GaN}}{\Omega_{alloy}} + \frac{\Omega_{GaAs}}{\Omega_{alloy}}(1-x)x(1-y)\right]V_{GaN}(r) + \left[xy(1-x)\frac{\Omega_{InN}}{\Omega_{alloy}} + (1-x)^2y\frac{\Omega_{InAs}}{\Omega_{alloy}}\right]V_{InAs}(r) + \left[(1-x)x(1-y)\frac{\Omega_{GaN}}{\Omega_{alloy}} + (1-x)^2(1-y)\frac{\Omega_{GaAs}}{\Omega_{alloy}}\right]V_{GaAs}(r) \quad (11)$$

Where Ω_{alloy}, Ω_{InN}, Ω_{InAs}, Ω_{GaN} and Ω_{GaAs} are respectively the volumes of the alloy and the binary systems InN, InAs, GaN and GaAs. The non-periodic potentials V_{1dis} and V_{2dis} can be expressed as:

$$V_{1dis}(r) = -p_1[y(1-y)]^{0.5}\frac{1}{\Omega_{alloy}}\{[x^2\Omega_{InN} + x(1-x)\Omega_{InAs}]V_{InN(r)} + [x(1-x)\Omega_{InN} + (1-x)^2\Omega_{InAs}]V_{InAs(r)} - [x^2\Omega_{GaN} + x(1-x)\Omega_{GaAs}]V_{GaN(r)} - [x(1-x)\Omega_{GaN} + (1-x)^2\Omega_{GaAs}]V_{GaAs(r)}\} \quad (12)$$

$$V_{2dis}(r) = -p_2[x(1-x)]^{0.5}\frac{1}{\Omega_{alloy}}\{[y^2\Omega_{InN} + y(1-y)\Omega_{GaN}]V_{InN(r)} + [y(1-y)\Omega_{InN} + (1-y)^2\Omega_{GaN}]V_{GaN(r)} - [y^2\Omega_{InAs} + y(1-y)\Omega_{GaAs}]V_{InAs(r)} - [y(1-y)\Omega_{InAs} + (1-y)^2\Omega_{GaAs}]V_{GaAs(r)}\} \quad (13)$$

The disorder parameters p_1 and p_2 are varied until agreement is achieved with the BAC model predictions. Our quaternaries have been studied mainly for N-content $0 \leq y \leq 0.03$, a range where we expect to get good optical qualities of the GaInAsN thin films.

RESULTS AND DISCUSSION

The results for Polarity, α_p, covalency, α_c, heavy hole and electron effective masses, m_h and m_e of GaInAsN for different compositions of x and y are as shown in Table 1.

Table 1: Polarity, α_p, Covalency, α_c, Heavy Hole and Electron Effective Masses, m_h and m_e of GaInAsN for Different Compositions of x and y

Semiconductor Material	α_p	α_c	$m_h(m_0)$	$m_e(m_0)$	$\mu\ (m_0)$
$InAs$	0.5200	0.8542	0.3333	0.0340	0.0309
$Ga_{0.3}In_{0.7}As$	0.4235	0.9059	0.3381	0.0420	0.0374
$Ga_{0.7}In_{0.3}As$	0.3181	0.9481	0.3446	0.0552	0.0476
$Ga_{0.3}In_{0.7}As_{0.99}N_{0.01}$	0.4295	0.9031	0.3381	0.0454	0.0374
$Ga_{0.3}In_{0.7}As_{0.97}N_{0.03}$	0.4414	0.8973	0.3381	0.0492	0.0374
$Ga_{0.7}In_{0.3}As_{0.99}N_{0.01}$	0.3221	0.9467	0.3446	0.0650	0.0476
$Ga_{0.7}In_{0.3}As_{0.97}N_{0.03}$	0.3301	0.9439	0.3446	0.0724	0.0476
$GaAs$	0.2524	0.9676	0.3497	0.0670	0.0562

As can be seen from table 1, our theoretical investigation into the exciton characteristics of dilute GaInAsN semiconductors indicates that the polarity, covalency, heavy hole, and electron effective masses are all greatly impacted by the addition of nitrogen. The polarity of excitons is altered due to changes in the electrostatic interactions introduced by nitrogen, influencing exciton stability. The covalency of the material is modified, affecting the strength of the electron-hole binding. The heavy hole effective mass is impacted by nitrogen-induced band structure changes, affecting exciton dynamics.

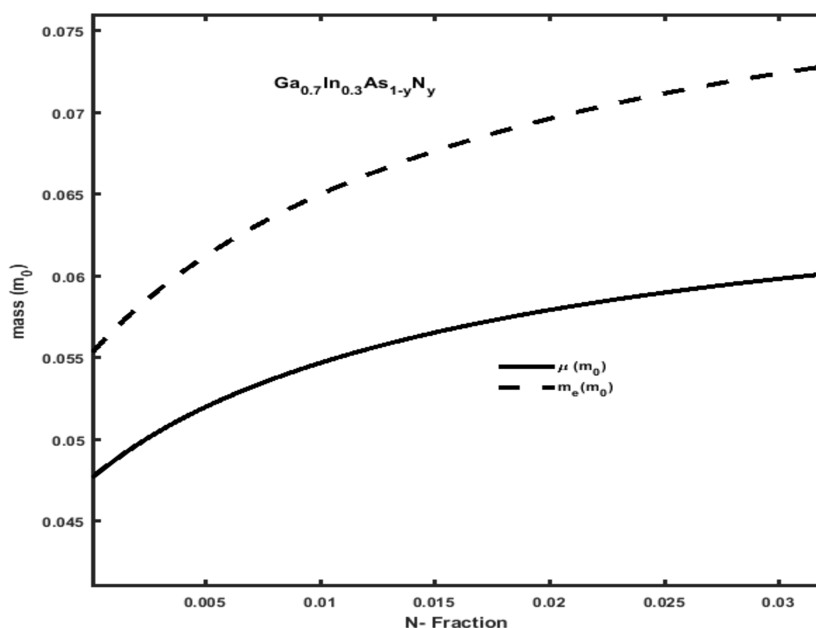

Figure 1: Effective Masses Versus Compositions N-fraction for $Ga_{0.7}In_{0.3}As_{1-y}N_y$.

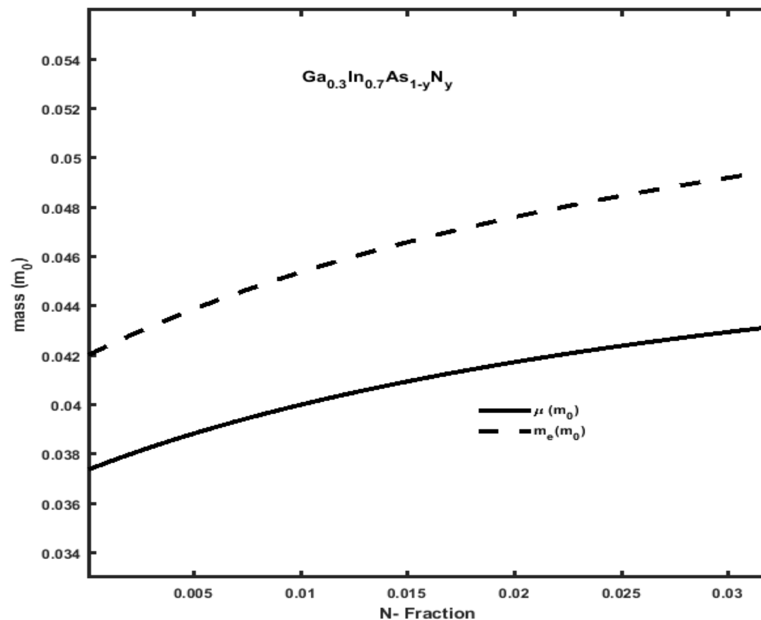

Figure 2: Effective Masses Versus Compositions N-fraction for $Ga_{0.3}In_{0.7}As_{1-y}N_y$

Similarly, figures 1 and 2 provide a comprehensive overview of the electron and reduced effective masses for various GaInAsN compositions. These parameters help in the understanding of the electronic and optical properties of these semiconductors. These plots of electron and reduced effective masses against nitrogen fractions reveals significant trends that impact the electronic and optical properties of GaInAsN semiconductors. The increase in electron effective mass with higher nitrogen content reflects enhanced perturbations in the conduction band, while the behavior of the reduced effective mass depends on the combined effects of electron and hole effective masses. The electron effective mass is altered, influencing exciton properties such as binding energy and spatial extent. Nitrogen incorporation introduces localized states and strain into the crystal lattice, which perturb the conduction band structure. This perturbation typically leads to a heavier electron effective mass. The observed increase in electron effective masses with higher nitrogen fractions is a reflection of this enhanced perturbation and strain. This is in agreement with the reported literature in Shhri *et al.* (2011) and Bouarissa and Saib (2010). These modifications are critical for understanding and optimizing the performance of GaInAsN-based optoelectronic devices.

Table 2: Refractive Index, Static and High Frequency Dielectric Constants, of GaInAsN for Different Compositions of x and y

Semiconductor Material	n		ε_0		ε_∞	
	This work	Others	This work	Others	This work	Others
$InAs$	3.8608	3.91	23.5906	16.33	14.9058	14.91
$Ga_{0.3}In_{0.7}As$	3.7250		18.4030	15.17	13.8756	13.86
$Ga_{0.7}In_{0.3}As$	3.4611		13.9033	13.09	11.9794	11.97
$Ga_{0.3}In_{0.7}As_{0.99}N_{0.01}$	3.7815		19.1512		14.2994	
$Ga_{0.3}In_{0.7}As_{0.97}N_{0.03}$	3.8687		20.4460		14.9665	
$Ga_{0.7}In_{0.3}As_{0.99}N_{0.01}$	3.5403		14.6140		12.5335	
$Ga_{0.7}In_{0.3}As_{0.97}N_{0.03}$	3.6447		15.6288		13.2835	
$GaAs$	3.2011	3.21	11.2124	11.21	10.2472	10.26

Table 2 shows the results obtained for refractive index, static and high-frequency dielectric constants in this work. These results were graphically analysed in figures 3, 4, and 5 respectively. They show how nitrogen incorporation modifies these key optical properties which are in accordance with the results obtained by Shhri *et al.,* (2011). The changes in the refractive index reflect the alterations in light propagation, while the variations in static and high-frequency dielectric constants reveal insights into exciton dynamics. These findings are essential for optimizing the design and performance of optoelectronic devices using GaInAsN.

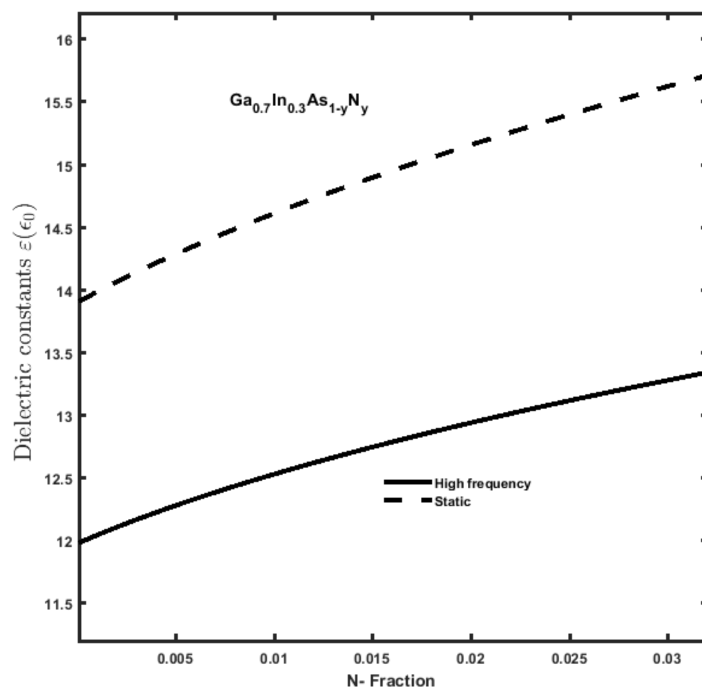

Figure 3: Dielectric Constants Versus Compositions N-fraction for $Ga_{0.7}In_{0.3}As_{1-y}N_y$

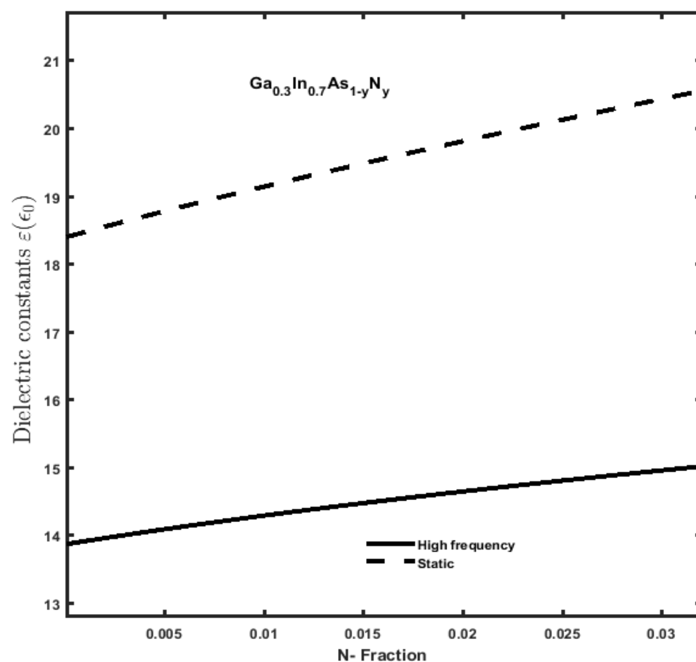

Figure 4: Dielectric Constants Versus Compositions N-fraction for $Ga_{0.3}In_{0.7}As_{1-y}N_y$

Figures 3 and 4 showed the trends in static and high-frequency dielectric constants as functions of nitrogen fraction for various GaInAsN alloys. The plot of static and high-frequency dielectric constants versus nitrogen fraction reveals that nitrogen incorporation generally increases the dielectric constants of GaInAsN alloys. The static dielectric constant shows a more pronounced increase with nitrogen content, reflecting enhanced polarization effects, while the high-frequency dielectric constant also increases but to a slightly lesser degree. These insights are valuable for tailoring semiconductor materials for specific optical and electronic applications, providing a basis for designing materials with optimized dielectric properties.

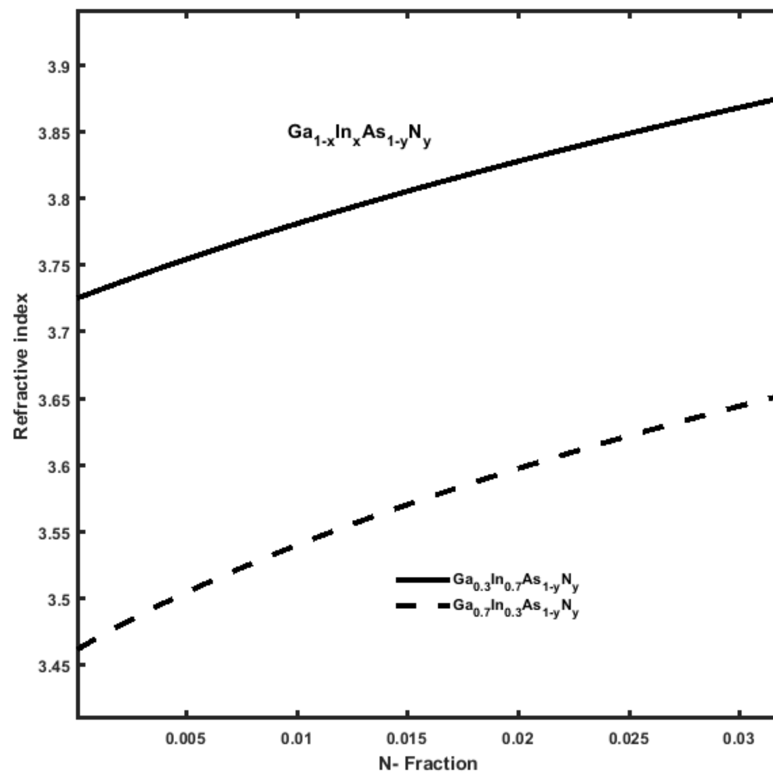

Figure 5: Refractive index Versus Compositions N-fraction for $Ga_{1-x}In_xAs_{1-y}N_y$

Figure 5 is the plot of the refractive index as a function of nitrogen fraction for various GaInAsN compositions. This plot of the refractive index versus nitrogen fraction reveals that nitrogen incorporation into GaInAs alloy generally increased the refractive index, with a more pronounced effect at higher nitrogen concentrations. This relationship provides valuable insight into the design of semiconductor materials with tailored optical properties. The nitrogen fractions and alloy compositions were carefully selected. By doing this, one can optimize materials for specific optical applications and enhance performance in photonic and optoelectronic devices.

Table 3: Calculated Exciton Parabolic and Non-parabolic Binding Energy, Bohr Radius and Reduced Mass

Semiconductor Material	E_B (meV)		Literature	a_B (Å)	
	Parabolic approx.	Non-parabolic approx.		This work	others
$InAs$	-0.7540	-0.7555	-1.56	404.4806	355.1
$Ga_{0.3}In_{0.7}As$	-1.4999	-1.5034	-2.14	260.6477	
$Ga_{0.7}In_{0.3}As$	-3.3469	-3.3568	-3.78	154.6102	
$Ga_{0.3}In_{0.7}As_{0.99}N_{0.01}$	-1.4836	-1.4877		253.2075	
$Ga_{0.3}In_{0.7}As_{0.97}N_{0.03}$	-1.3977	-1.4028		251.7541	
$Ga_{0.7}In_{0.3}As_{0.99}N_{0.01}$	-3.4827	-3.4948		141.3536	
$Ga_{0.7}In_{0.3}As_{0.97}N_{0.03}$	-3.3324	-3.3460		138.1359	
$GaAs$	-6.0824	-6.1051	-6.27	105.4916	116.1

From Table 3, it is evident that our study of exciton properties in dilute GaInAsN semiconductors reveals notable effects of nitrogen incorporation. The comparison between non-parabolic and parabolic binding energies shows that nitrogen alters the exciton interactions, leading to increased binding energies due to the modified band structure (Uwaoma *et al.,* 2024).

The relatively small exciton binding energy implies a large Bohr radius with a large spatial separation of the electrons and holes. This can be clearly seen from our results concerning the exciton Bohr radius in $Ga_{1-x}In_xAs_{1-y}N_y$. We also included in Table 1, the value of α_B in InAs and GaAs respectively reported in (Bhardwaj and Das, 2016). Which is in good

accordance between our result and that reported in the literature and can be observed. Note that the exciton Bohr radius decreases monotonically with increase in the composition x and y.

Also, the Bohr radius calculations indicate that the spatial extent of the exciton changes with nitrogen concentration, reflecting variations in effective masses and dielectric environment. Similarly, the reduced mass of the exciton is modified, affecting its stability and interaction strength. These results explain the significant impact of nitrogen on exciton properties, which is crucial for optimizing the performance of optoelectronic devices based on GaInAsN.

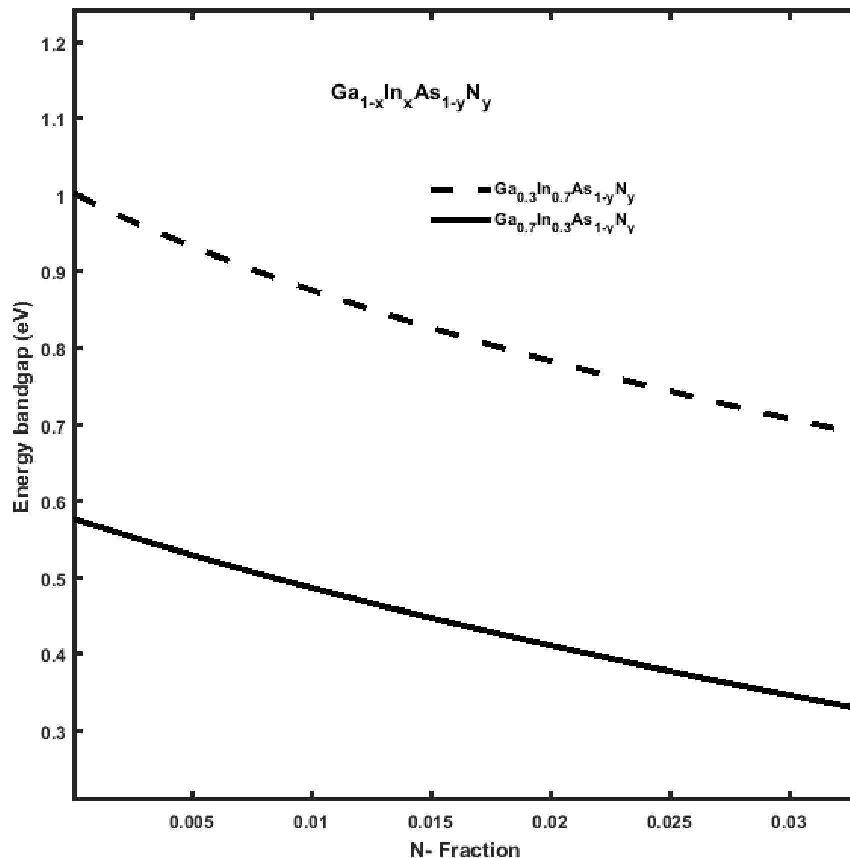

Figure 6: Energy band gap Versus N-fraction for $Ga_{1-x}In_xAs_{1-y}N_y$

Figure 6 is a plot of energy band gap Versus N-fraction for $Ga_{1-x}In_xAs_{1-y}N_y$**.** Considering the variation of the bandgap energy as a function of N fractions, the bandgap value decreases when the N fractions increase. This implies that the bandgap value of the quaternary alloy is always low. For example, using In fraction of 5% the bandgap value of the quaternary alloy is 1.05 eV, leading to a decrease. For the corresponding quaternary alloy (with here 3% of N fraction), the bandgap is significantly lower than in the ternary cases. It is then clear that N fraction has much important effect on the bandgap value thanIn. Evidently, In and N fractions reduce both bandgap values. A good agreement between experimental and theoretical results concerning this quaternary alloy family is observed for low to moderate nitrogen concentration values (Uwaoma *et al.,* 2024). For high value of nitrogen concentration, a large discrepancy is noticed. This has been linked to the amount of dislocations arising in the real material (Aissat *et al.,* 2015).

CONCLUSION

A theoretical study of the exciton properties of dilute GaInAsN semiconductors have been delivered, starting with the empirical pseudopotential method under the VCA approximation, the alloy disorder effects due to In and N incorporation were considered. Similar modifications were observed in the optoelectronic properties; the hole effective mass, m_h, electron effective mass, m_e, binding energy, E_B, Bohr radius, α_B, polarity, α_p, covalence, α_c, reduced mass, μ, high frequency dielectric constant, ε_∞, static dielectric constant, ε_0 and the refractive index n. These modifications reflect in the variation in the exciton

binding energies E_B. For all the alloy composition studied, it was observed that the binding of the exciton varies between the values for InAs~ 0.7540 meV and GaAs $\sim 6.0824\ meV$. The corresponding exciton Bohr radii values for InAs~ 404.4806 Åand GaAs~ 105.4916 Å. The effect of the alloy composition (x and y) on the exciton properties of dilute GaInAsN semiconductors were studied in four different substrates. The underlying physical mechanisms of the quaternary semiconductor are hence presented. However, in the case of GaInAsN, non-parabolicity arising from the complex band structure and the incorporation of nitrogen introduces significant deviations. Our results indicate that the non-parabolic binding energy more accurately captures the physical realities of the system, particularly at higher energy states where band non-parabolicity becomes pronounced. This distinction is crucial for precise modeling and prediction of excitonic behavior in real-world applications. The analysis of polarity and covalency offers insights into the chemical bonding nature within the GaInAsN matrix, revealing a delicate balance between ionic and covalent character that influences the material's optical and electronic properties. The refractive index and dielectric constants, both static and high-frequency, further elaborate on the interaction of electromagnetic waves with the semiconductor, which is pivotal for the design of optoelectronic devices.

REFERENCES

Baaziz, H., Charifi, Z., Reshak, A., Hamad, B. and Al-Douri Y. (2012). Structural and electronic properties of GaN_xAs_{1-x} alloys. *Journal of Applied Physics A*, 106, 687-696

Bhardwaj, P. and Das N. (2016). Exciton binding energy in bulk and Quantum well of semiconductors with non-parabolic energy bands. *International Journal of Engineering sciences and Research Technology*. 5, (11).

Bouarissa, N. and Boucenna, M. (2009). Band parameters for AlAs, InAs and their ternary mixed crystals. *Journal of the Royal Swedish Academy of Sciences PhysicaScripta*, 79. 015-701.

Bouarissa, N. and Saib, S. (2010). AB INITIO study of lattice vibration and polaron properties in zinc-blende $Al_xGa_{1-x}N$ alloys.*Journal Applied Physics,* 108, 113710.

Chiesa, M., Livraghi, S., Paganini, M.C., Salvadori, E. and Giamello, E. (2020). Nitrogen-doped semiconducting oxides. Implications on photochemical, photocatalytic and electronic properties derived from EPR spectroscopy. *Journal of Chemical Science,* 11, 6623-6641.

Güngerich, M., Klar, P.J., Heimbrodt, W., Volz, K., Köhler, K., Wagner, J., Polimeni, A., Capizzi, M., and Gomeniuk, Y.V. (2006). Correlation of band formation and local vibrational mode structure in $Ga_{0.95}Al_{0.05}As_{1-x}N_x$ with $0 \leq x \leq 0.03$. *Physica Status Solidi,* 10, 1002.

Harrison, P. and Valavanis, A. (2016). *Quantum wells, wires and dots: Theoretical and computational Physics of semiconductor nanostructures*. John Wiley & sons. Ltd.

Hwaug, H. and Koch, S. W. (2009). *Quantum theory of the optical and electronic properties of semiconductors.* 5th edition, World scientific Publishing Company Plc. Ltd, Singapore. 484.

Koksal, K. and Sahin, M. (2012). The effect of dilute nitrogen on nonlinear optical properties of the InGaAsN/GaAs single quantum wells. *The European Physical Journal B*. 85, 333.

Lin, H. and Singh, J. (2009). Electronic and optical properties of InGaN quantum dot based light emitters for solid state lighting, *Journal of applied physics,* 105, 013-117.

Merabet, B., Lachebi, A. and Abid, H. (2011). Effect of nitrogen incorporation on the electronic and optical properties of AlGaAsN/GaAs quantum well lasers. *Turkish Journal of Physics*. 35, 13 – 22.

Perkins, J.D., Mascarenhas, A., Zhang, Y., Geisz, J.F., Friedman, D.J., Oslon, J.M., and Kurtz, S.R. (1999). Nitrogen-Activated Transitions, Level Repulsion, and Band Gap Reduction in $GaAs_{1-x}N_x$ with $x<0.03$. *Physics Review Letter*. 82, 3312.

Potter, R.J. and Balkan, N. (2004).Optical properties of GaNAs and GaInAsN quantum wells. *Journal of Physics: Condensed Matter*. 16, S33-87.

Shan, W., Walukiewicz, W., III, J.W.A., Haller, E.E., Geisz, J.F., Friedman, D.J., Oslon, J.M., and Kurtz, S.R. (1999). Band Anticrossing in GaInNAs Alloys. *Physical Review Letters*. 82, 1221-1224.

Shhri, H. A., Bouarissa, N. and Khan, M. A. (2011). Exciton and polaron properties in $Ga_xIn_{1-x}As$ ternary mixed crystals. *Journal of Luminescence,* 131, 2153-2159.

Stier, O., Grundmann, M. and Bimberg, D. (2017), Electronic and optical properties of strained quantum dots modeled by 8-band k.p theory. *Physical Review B*. 59, 5688-5701.

Suemune, I., Uesugi, K. and Walukiewicz, W. (2000). Role of nitrogen in the reduced temperature dependence of band-gap energy in GaNAs. *Applied Physics Letter*. 77, 3021-3023.

Uma, P. M., Peter, A.J., Chang Woo, L. and Duque, C.A. (2016).Interband emission energy in a dilute nitride quaternary semiconductor quantum dot for longer wavelength applications. *Journal of Physica E: Low-dimensional Systems and Nanostructures*. 81, 102-107.

Uwaoma, C.J., Oriaku, C.I. and Ugochukwu J. (2024). Exciton binding energies of dilute quaternary GaInAsN alloy semiconductors. *Maiden Research and Innovation Fair/Conference*, Directorate of University Research and Administration, Michael Okpara University of Agriculture, Umudike, Pp. 499-508.

Wang, Q. H., Kalantar-Zadeh, K., Kis, A., Coleman, J. N. and Strano, M. S. (2012). Electronics and optoelectronics of Two-Dimensional Transition Metal Dichalcogenides. *Journal of Nature Nanotechnology*. 7, 699-712.